



**HAL**  
open science

# A Galerkin approach to FFT-based homogenization methods

Sébastien Brisard, Luc Dormieux

► **To cite this version:**

Sébastien Brisard, Luc Dormieux. A Galerkin approach to FFT-based homogenization methods. 6th European Congress on Computational Methods in Applied Sciences and Engineering, ECCOMAS 2012, Sep 2012, Vienna, Austria. pp.1709-1718. hal-00738040

**HAL Id: hal-00738040**

**<https://enpc.hal.science/hal-00738040>**

Submitted on 18 Sep 2015

**HAL** is a multi-disciplinary open access archive for the deposit and dissemination of scientific research documents, whether they are published or not. The documents may come from teaching and research institutions in France or abroad, or from public or private research centers.

L'archive ouverte pluridisciplinaire **HAL**, est destinée au dépôt et à la diffusion de documents scientifiques de niveau recherche, publiés ou non, émanant des établissements d'enseignement et de recherche français ou étrangers, des laboratoires publics ou privés.

## A GALERKIN APPROACH TO FFT-BASED HOMOGENIZATION METHODS

Sébastien Brisard<sup>1</sup> and Luc Dormieux<sup>2</sup>

<sup>1,2</sup>Université Paris-Est, Laboratoire Navier  
(UMR Ecole des Ponts ParisTech – IFSTTAR – Université Paris-Est Marne la Vallée)  
Ecole des Ponts ParisTech  
6-8 avenue Blaise Pascal  
F-77455, Marne la Vallée, France  
<sup>1</sup>e-mail: sebastien.brisard@ifsttar.fr  
<sup>2</sup>e-mail: luc.dormieux@enpc.fr

**Keywords:** fast Fourier transform, Galerkin approximation, linear elasticity, polarization

**Abstract.** *Since their introduction by Moulinec and Suquet [1, 2], FFT-based full-field simulations of the mechanical properties of composites have become increasingly popular, with applications ranging from the linear elastic behaviour of cementitious materials [3], to the plasticity of polycrystals [4].*

*Recently, the authors have proposed [5] a new formulation of these numerical schemes, based on the energy principle of Hashin and Shtrikman [6]. While similar in principle to the original scheme of Moulinec and Suquet, the new scheme was shown to be much better-behaved. Indeed, convergence of the scheme is guaranteed for any contrast, without having to resort to augmented Lagrangian approaches [7]. Besides, convergence of the new scheme is generally much faster. However, the new scheme has two drawbacks. First, the reference material must be stiffer (or softer) than all constituents of the composite; this is not always possible, for example when the composite contains both pores and rigid inclusions. Second, the scheme requires the preliminary computation of the so-called consistent Green operator, which turned out to be a difficult task in three dimensions.*

*In order to relax these requirements, an in-depth mathematical analysis of these schemes was carried out by the authors [8].*

*In this paper, the Lippmann-Schwinger equation and its variational form will briefly be recalled. The Galerkin approach will then be adopted for the discretization of this equation, and it will be shown that the basic scheme of [1] as well as the energy scheme proposed in [5] can both be viewed as well-posed Galerkin approximations of the Lippmann-Schwinger equation.*

*Contrary to what was previously believed [7, 5] these approximations are convergent, regardless of the reference material (provided that its stiffness is positive definite). Comparison of these two approximations leads to the derivation of the so-called filtered, non-consistent approach, which combines the assets of the two former methods.*

*Finally, some applications will be shown. In particular, the important problem of heterogeneous voxels will be addressed.*

# 1 THE LIPPMANN-SCHWINGER EQUATION AND ITS VARIATIONAL FORM

## 1.1 From the local problem of elasticity to the Lippmann-Schwinger equation

This paper is devoted to the homogenization of linear elastic materials with periodic microstructures. Let  $\Omega = (0, L_1) \times \cdots \times (0, L_d)$  be the unit-cell, and  $\mathbf{C}(\mathbf{x})$  the local stiffness tensor. Periodic homogenization requires the solution to the following local problem on the unit-cell

$$\operatorname{div} \boldsymbol{\sigma} = \mathbf{0}, \quad (1a)$$

$$\boldsymbol{\sigma}(\mathbf{x}) = \mathbf{C}(\mathbf{x}) : \boldsymbol{\varepsilon}(\mathbf{x}), \quad (1b)$$

$$2\varepsilon_{ij}(\mathbf{x}) = \partial_i u_j(\mathbf{x}) + \partial_j u_i(\mathbf{x}), \quad (1c)$$

$$\mathbf{u}(\mathbf{x} + L_i \mathbf{e}_i) = \mathbf{u}(\mathbf{x}) + L_i \mathbf{E} \cdot \mathbf{e}_i, \quad (1d)$$

$$\boldsymbol{\sigma}(\mathbf{x} + L_i \mathbf{e}_i) \cdot \mathbf{e}_i = \boldsymbol{\sigma}(\mathbf{x}) \cdot \mathbf{e}_i, \quad (1e)$$

where  $\mathbf{E}$  is the macroscopic (imposed) strain,  $\mathbf{x} \in \mathbb{R}^d$ ,  $i, j = 1, \dots, d$  and  $\mathbf{e}_1, \dots, \mathbf{e}_d$  denote the basis vectors (no summation on repeated indices in the above expressions). The macroscopic elastic properties are then given by

$$\mathbf{C}^{\text{eff}} : \mathbf{E} = \overline{\mathbf{C} : \boldsymbol{\varepsilon}},$$

where  $\boldsymbol{\varepsilon}(\mathbf{x})$  solves problem (1) (overlined quantities denote volume averages on  $\Omega$ ). Finding  $\boldsymbol{\varepsilon}$  is equivalent to solving the following integral equation, known as the Lippmann-Schwinger equation [9, 10]

$$(\mathbf{C} - \mathbf{C}_0)^{-1} : \boldsymbol{\tau} + \Gamma_0 * \boldsymbol{\tau} = \mathbf{E}, \quad (2)$$

where  $\Gamma_0$  is the so-called Green operator for strains [11], associated with the reference material  $\mathbf{C}_0$ . In the above equation,  $*$  stands for the convolution product, which reads in Fourier space<sup>1</sup>

$$(\Gamma_0 * \boldsymbol{\tau})(\mathbf{x}) = \sum_{\mathbf{b} \in \mathbb{Z}^d} \hat{\Gamma}_0(\mathbf{k}_b) : \hat{\boldsymbol{\tau}}(\mathbf{k}_b) \exp(i\mathbf{k}_b \cdot \mathbf{x}),$$

with

$$\mathbf{k}_b = \frac{2\pi b_1}{L_1} \mathbf{e}_1 + \cdots + \frac{2\pi b_d}{L_d} \mathbf{e}_d, \quad \text{for } \mathbf{b} \in \mathbb{Z}^d,$$

and [10]

$$\hat{\Gamma}_{0,ijkl}(\mathbf{k}) = \frac{1}{4\mu_0} (\delta_{ih} n_j n_l + \delta_{il} n_j n_h + \delta_{jh} n_i n_l + \delta_{jl} n_i n_h) - \frac{1}{2\mu_0(1-\nu_0)} n_i n_j n_h n_l,$$

where  $\mathbf{n} = \mathbf{k}/\|\mathbf{k}\|$  and  $\mu_0$  (resp.  $\nu_0$ ) is the shear modulus (resp. Poisson ratio) of the isotropic reference material.

The purpose of this paper is the mathematical analysis of two numerical schemes, namely the non-consistent scheme of Moulinec and Suquet [1, 2] and the consistent scheme of Brisard and Dormieux [5].

<sup>1</sup>In this paper, *greek* multi-indices ( $\beta \in \mathbb{Z}^d$ ) refer to the *real* space, while *latin* multi-indices ( $\mathbf{b} \in \mathbb{Z}^d$ ) refer to the Fourier space.

## 1.2 Variational formulation of the Lippmann-Schwinger equation

This formulation can be found by point-wise multiplication of (2) with a test function  $\varpi(\boldsymbol{x})$  (second rank, symmetric tensor), and integration over the unit-cell  $\Omega$ . The following variational problem results

$$\text{Find } \boldsymbol{\tau} \in \mathbb{V} \text{ such that } a(\boldsymbol{\tau}, \boldsymbol{\varpi}) = \ell(\boldsymbol{\varpi}) \text{ for all } \boldsymbol{\varpi} \in \mathbb{V}, \quad (3a)$$

where

$$a(\boldsymbol{\tau}, \boldsymbol{\varpi}) = \overline{\boldsymbol{\varpi} : (\boldsymbol{C} - \boldsymbol{C}_0)^{-1} : \boldsymbol{\tau}} + \overline{\boldsymbol{\varpi} : (\boldsymbol{\Gamma}_0 * \boldsymbol{\tau})}, \quad \ell(\boldsymbol{\varpi}) = \boldsymbol{E} : \boldsymbol{\varpi}, \quad (3b)$$

and the appropriate choice for  $\mathbb{V}$  is the space of second rank, symmetric tensors with square integrable components. Under some assumptions, which are stated in [8], it can be shown that this variational problem is well-posed in the sense of Hadamard [12]. In particular, this problem has a unique solution  $\boldsymbol{\tau} \in \mathbb{V}$  for any macroscopic strain  $\boldsymbol{E}$  and reference material  $\boldsymbol{C}_0$ . That this result is true regardless of the reference material is of paramount importance. It should be noted that in [8], well-posedness could not be proved for porous materials; this important special case is currently under investigation.

## 2 DISCRETIZATION OF THE LIPPMANN-SCHWINGER EQUATION

### 2.1 Galerkin approximation

A Galerkin approximation of problem (3) requires the selection of a finite-dimension subspace  $\mathbb{V}^h \subset \mathbb{V}$  on which the following variational problem is solved

$$\text{Find } \boldsymbol{\tau}^h \in \mathbb{V}^h \text{ such that } a^h(\boldsymbol{\tau}^h, \boldsymbol{\varpi}^h) = \ell(\boldsymbol{\varpi}^h) \text{ for all } \boldsymbol{\varpi}^h \in \mathbb{V}^h, \quad (4)$$

where  $a^h$  approximates in some sense the bilinear form  $a$ .

In the present paper,  $\mathbb{V}^h$  is defined as the space of cell-wise constant polarizations. More precisely, we assume that the unit cell can be divided in  $N = N_1 \times \dots \times N_d$   $d$ -dimensional cubic cells, with size  $h = \frac{L_1}{N_1} = \dots = \frac{L_d}{N_d}$ . Cells are indexed by  $\beta$ , with  $0 \leq \beta_i < N_i$ ,  $i = 1, \dots, d$ ; the domain occupied by cell  $\beta$  is denoted  $\Omega_\beta^h \subset \Omega$ , and the constant value of  $\boldsymbol{\tau}^h \in \mathbb{V}^h$  (resp.  $\boldsymbol{\varpi}^h \in \mathbb{V}^h$ ) over cell  $\beta$  is denoted  $\boldsymbol{\tau}_\beta^h$  (resp.  $\boldsymbol{\varpi}_\beta^h$ ).

The approximate bilinear function  $a^h$  must then be selected so as to ensure that problem (4) is well-posed, and  $\boldsymbol{\tau}^h \rightarrow \boldsymbol{\tau}$  in the  $L^2$  sense as  $h \rightarrow 0$ . It is consistent [12] if  $a^h$  can be extended to  $\mathbb{V} \times \mathbb{V}^h$ , and

$$\text{For all } \boldsymbol{\varpi}^h \in \mathbb{V}^h, \quad a^h(\boldsymbol{\tau}, \boldsymbol{\varpi}^h) = \ell(\boldsymbol{\varpi}^h),$$

where  $\boldsymbol{\tau} \in \mathbb{V}$  is the unique solution to problem (3).

It should first be noted that only the non-local part of  $a$ —the convolution product in (3b)—is approximated, since the local part can easily be evaluated on  $\mathbb{V}^h$ . Indeed

$$\text{For all } \boldsymbol{\tau}^h, \boldsymbol{\varpi}^h \in \mathbb{V}^h, \quad \overline{\boldsymbol{\varpi}^h : (\boldsymbol{C} - \boldsymbol{C}_0)^{-1} : \boldsymbol{\tau}^h} = \frac{1}{N} \sum_{\beta_1=0}^{N_1-1} \dots \sum_{\beta_d=0}^{N_d-1} \boldsymbol{\varpi}_\beta^h : (\boldsymbol{C}_\beta^h - \boldsymbol{C}_0)^{-1} : \boldsymbol{\tau}_\beta^h,$$

<sup>2</sup>An approximate linear form  $\ell^h$  might have been used as well. However, the exact linear form  $\ell$  defined by (3b) is very simple, and will always be computed exactly on  $\boldsymbol{\tau}^h$ .

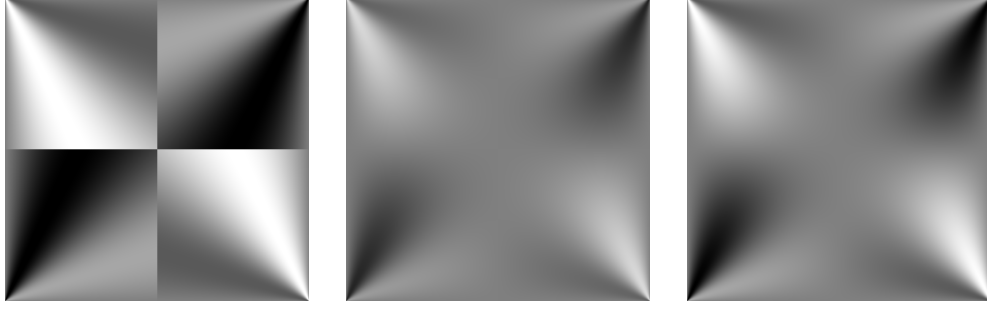


Figure 1: Graphical representation of the  $xxy$  component of the non-consistent (left), consistent (middle) and filtered, non-consistent discrete Green operators in plane elasticity ( $\nu_0 = 0.3$ ). The consistent and filtered non-consistent operators are smooth, while the non-consistent operator exhibits a sharp discontinuity at high frequencies.

where  $\mathbf{C}^h(\mathbf{x})$  is the cell-wise constant stiffness whose value on cell  $\beta$  is defined by the following volume average

$$(\mathbf{C}_\beta^h - \mathbf{C}_0)^{-1} = \frac{1}{|\Omega_\beta^h|} \int_{x \in \Omega_\beta^h} [\mathbf{C}(\mathbf{x}) - \mathbf{C}_0]^{-1} d\Omega. \quad (5)$$

As for the non-local part of  $a$ , it is approximated as follows

$$\overline{\boldsymbol{\varpi}^h : (\Gamma_0^h * \boldsymbol{\tau}^h)} = \frac{1}{N} \sum_{\beta_1=0}^{N_1-1} \cdots \sum_{\beta_d=0}^{N_d-1} \boldsymbol{\varpi}_\beta^h : \text{DFT}_\beta^{-1} \left[ \hat{\Gamma}_{0,b}^h : \text{DFT}_b(\boldsymbol{\tau}^h) \right],$$

where DFT denotes the  $d$ -dimensional discrete Fourier transform, and  $\Gamma_{0,b}^h$  is the discretized Green operator in Fourier space, to be defined below. It should be noted that the DFT involves only finite sums (as opposed to infinite Fourier series).

In what follows, the original method of Moulinec and Suquet [1, 2] and the newer method proposed in [5] are both formulated in the framework of Galerkin approximations involving two different approximations  $\Gamma_0^h$  of the Green operator  $\Gamma_0$  (namely, the non-consistent discrete Green operator  $\Gamma_0^{h,\text{nc}}$ , and the consistent discrete Green operator  $\Gamma_0^{h,\text{c}}$ ). Finally, the filtered non-consistent discrete Green operator  $\Gamma_0^{h,\text{fnc}}$  is introduced; it combines the assets of both non-consistent and consistent operators.

It is shown in [8] that regardless of the reference material  $\mathbf{C}_0$ , problem (4) resulting from any of these three discrete Green operators is well-posed (in particular, it always has a unique solution). Besides, these discrete Green operators are asymptotically consistent in the sense of [12, definition 2.15]. This ensures the convergence of the approximate solution  $\boldsymbol{\tau}^h$  to the true solution  $\boldsymbol{\tau}$  as  $h \rightarrow 0$ .

To close this section, it is noted that regardless of the discrete Green operator  $\Gamma_0^h$ , the discretized problem (4) always leads to a linear system, the matrix of which is generally full. However, as noted in [1, 2, 5], products involving this matrix can be computed efficiently by use of the fast Fourier transform. This advocates that iterative linear solvers [13] be used. Moulinec and Suquet [1, 2] use Neumann (fixed-point) iterations to solve (4), but this iterative scheme does not always converge [7] (although the system is always invertible). In [5, 8], more general iterative solvers like conjugate gradient, SYMMLQ [14] or LSQR [15] have been used: these solvers generally require less iterations to converge to the solution  $\boldsymbol{\tau}^h$  of (4).

## 2.2 The non-consistent approach

It can be shown [8] that the numerical scheme proposed by Moulinec and Suquet [1, 2] corresponds to the following non-consistent discretization of the Green operator,  $\Gamma_0^{h,nc}$

$$\hat{\Gamma}_{0,\mathbf{b}}^{h,nc} = \hat{\Gamma}_0(\mathbf{k}_{\mathbf{b}+n\mathbf{N}}), \quad 0 \leq b_i < N_i, \quad i = 1, \dots, d, \quad (6)$$

where  $\mathbf{b} + n\mathbf{N}$  denotes the multi-index  $(b_1 + n_1N_1, \dots, b_d + n_dN_d)$  and  $n_i = 0, 1$  so that the following inequality is verified

$$-\frac{N_i}{2} < b_i + n_iN_i \leq \frac{N_i}{2}.$$

In other words, the non-consistent discrete Green operator corresponds to the truncation of the true Green operator to the  $N_1 \times \dots \times N_d$  lowest frequencies.

## 2.3 The consistent approach

The bilinear form  $a(\boldsymbol{\tau}^h, \boldsymbol{\varpi}^h)$  can be computed *exactly* on the space  $\mathbb{V}^h$  of cell-wise constant polarizations [5]. This leads to the following consistent discretization of the Green operator,  $\Gamma_0^{h,c}$

$$\hat{\Gamma}_{0,\mathbf{b}}^{h,c} = \sum_{n_1=-\infty}^{+\infty} \dots \sum_{n_d=-\infty}^{+\infty} [F(h\mathbf{k}_{\mathbf{b}+n\mathbf{N}})]^2 \hat{\Gamma}_0(\mathbf{k}_{\mathbf{b}+n\mathbf{N}}), \quad 0 \leq b_i < N_i, \quad i = 1, \dots, d,$$

where

$$F(\mathbf{K}) = \text{sinc} \frac{K_1}{2} \dots \text{sinc} \frac{K_d}{2}.$$

The main asset of the consistent discrete Green operator is its ability to provide an upper-bound on the macroscopic elastic properties, provided that the reference material  $\mathbf{C}_0$  is stiffer than all phases in the composite. More precisely, as a result of the variational principle of Hashin and Shtrikman [16], if  $\mathbf{C}_0 - \mathbf{C}(\mathbf{x})$  is positive semidefinite for any  $\mathbf{x} \in \Omega$ , then

$$\frac{1}{2} \mathbf{E} : \mathbf{C}^{\text{eff}} : \mathbf{E} \leq \frac{1}{2} \mathbf{E} : \mathbf{C}_0 : \mathbf{E} + \frac{1}{2} \overline{\boldsymbol{\tau}^h} : \mathbf{E}, \quad (7)$$

where  $\boldsymbol{\tau}^h$  is the solution to (4), computed with  $\Gamma_0^{h,c}$ . Conversely, if  $\mathbf{C}_0 - \mathbf{C}(\mathbf{x})$  is negative semidefinite for any  $\mathbf{x} \in \Omega$ , then the above inequality is reversed. The use of FFT-based methods to produce bounds on the elastic properties of heterogeneous materials is illustrated in [5].

The consistent discrete Green operator is smoother than its non-consistent counterpart (figure 1, left and middle), resulting in better behaved approximate solutions  $\boldsymbol{\tau}^h$  (see 3.1). However, its computation is very difficult in three dimensions, as convergence of the above triple series is slow, and prone to catastrophic cancellations.

## 2.4 The filtered, non-consistent approach

In order to filter spurious high-frequencies, the so-called filtered, non-consistent discretized Green operator  $\Gamma_0^{h, \text{fnc}}$  was proposed in [8]

$$\hat{\Gamma}_{0,\mathbf{b}}^{h, \text{fnc}} = \sum_{n_1=-1,0} \dots \sum_{n_d=-1,0} [G(h\mathbf{k}_{\mathbf{b}+n\mathbf{N}})]^2 \hat{\Gamma}_0(\mathbf{k}_{\mathbf{b}+n\mathbf{N}}), \quad 0 \leq b_i < N_i, \quad i = 1, \dots, d,$$

where

$$G(\mathbf{K}) = \cos \frac{K_1}{4} \dots \cos \frac{K_d}{4}.$$

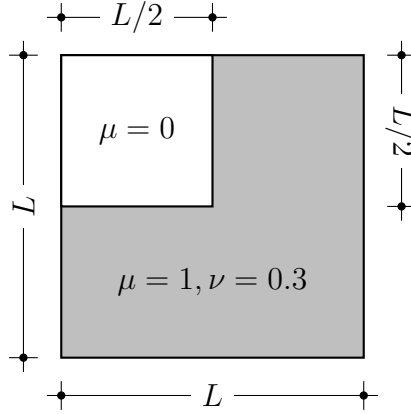


Figure 2: Geometry of the bidimensional (plane strain) problem solved in figure 3. The upper-left corner is a pore. The unit-cell is submitted to a macroscopic strain  $\mathbf{E} = \mathbf{e}_1 \otimes \mathbf{e}_2 + \mathbf{e}_2 \otimes \mathbf{e}_1$ .

Like the consistent discrete Green operator, the filtered non-consistent discrete Green operator is smooth; its computation is almost as easy as the non-consistent discrete Green operator of Moulinec and Suquet [1, 2].

### 3 APPLICATIONS

#### 3.1 Non-consistent vs. consistent approach

It is instructive to compare the three discrete Green operators. In the Fourier space, first, figure 1 shows the map of the  $xxxy$  component of the operators in plane strain elasticity. Clearly, the non-consistent operator exhibits a sharp discontinuity at high frequencies. This discontinuity is smoothed out by both the consistent and filtered, non-consistent discrete Green operators. Besides, these last two operators are very close, which means that the filtered non-consistent Green operator (whose computation is considerably simpler) can be advantageously substituted to the consistent Green operator.

In the real space, the discontinuity of the non-consistent discrete Green operator has a direct impact on the quality of the numerical solution  $\tau^h$ , which is polluted by a “checker-board” pattern as illustrated on figure 3, which represents the numerical solution to the problem sketched in figure 2, computed with the three different discrete Green operators. It is known that for heterogeneous materials containing voids, the Neumann solver of Moulinec and Suquet [1, 2] does not converge [7]. The conjugate gradient method was therefore used instead; this solver did converge to the unique solution of the discretized problem (4).

It should finally be noted that the numerical solutions found with the consistent and the filtered, non-consistent discrete Green operators are very close (see figure 3). A more quantitative analysis [8] in fact shows that using the latter instead of the former leads to negligible additional error on the  $L^2$ -norm  $\|\tau^h - \tau\|_{\mathbb{V}}$ . It is therefore recommended that the filtered, non-consistent discrete Green operator be systematically used.

#### 3.2 Heterogeneous voxels and finite resolution observations

Equation (5) is of high practical importance, because microstructures resulting from experimental observations are scarcely fully resolved. This means that in 3d reconstructions, voxels are not homogeneous. If the *composition* of each voxel can be assessed by other experimental means, then rule (5) might be applied to compute the best equivalent stiffness of each heterogeneous

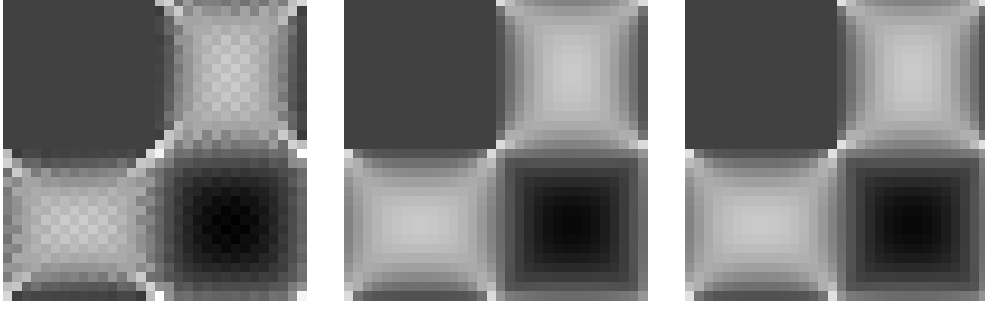


Figure 3: Map of  $\sigma_{xy}$  for the problem sketched in figure 2, computed on a  $32 \times 32$  grid, with the non-consistent (left), consistent (middle) and filtered, non-consistent (right) discrete Green operators. In all three computations, the reference material is the solid matrix.

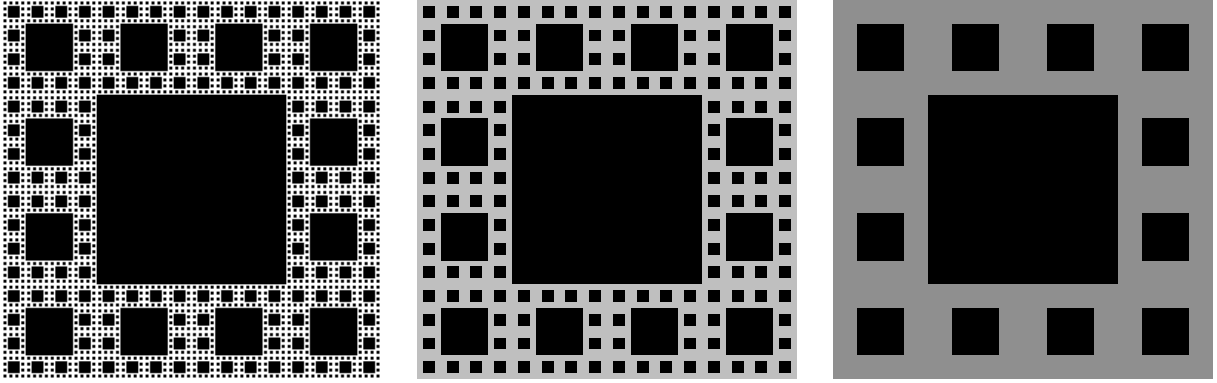


Figure 4: The multiscale porous microstructure, fully resolved (left). The total porosity is  $\varphi = 68.4\%$ , the smallest pores are two pixels wide, while the size of the overall microstructure is  $256 \times 256$  pixels. If the same microstructure is observed through a finite resolution instrument, then the smallest pores will no longer be fully resolved, and the largest pores will be embedded in a grayish porous matrix. For a  $4 \times 4$  resolution (middle), the porosity of the heterogeneous matrix is  $\varphi_m = 25\%$ ; for a  $16 \times 16$  resolution (right), the porosity of the heterogeneous matrix is  $\varphi_m = 43.75\%$ ;

voxels. Furthermore, application of this rule in combination with the consistent discrete Green operator guarantees that the resulting estimate of the macroscopic stiffness is in fact a *rigorous bound* [5].

This is illustrated below on a hypothetical multiscale porous microstructure, represented in figure 4. The elastic properties of the solid matrix (resp. the reference medium) are  $\mu = 1.0$ ,  $\nu = 0.3$  (resp.  $\mu_0 = 1.0$ ,  $\nu_0 = 0.3$ ). Since the reference material is stiffer than all phases, the result provides an upper-bound on the macroscopic elastic moduli. More precisely, (7) reads for  $\mathbf{E} = E_{12}(\mathbf{e}_1 \otimes \mathbf{e}_2 + \mathbf{e}_2 \otimes \mathbf{e}_1)$

$$4C_{1212}^{\text{eff}} E_{12}^2 \leq 2\mu_0 E_{12}^2 + \overline{\tau_{12}^h} E_{12},$$

where  $\tau^h$  is the approximate polarization field. The computation is first carried out on the fully resolved microstructure, then on a partially resolved microstructure.

### 3.3 Computation on fully resolved microstructures

On the fully resolved microstructure, each voxel in the computation grid is in fact homogeneous, and (5) is trivial. In order to allow for small-scale variations of the polarization field, the computation is carried out on a  $256 \times 256$  (initial grid), then  $512 \times 512$  and  $1024 \times 1024$  grid.

Grid size	Average polarization $\overline{\tau_{12}^h}$	Bound on $C_{1212}^{\text{eff}}$
16	-2.823	0.044
64	-2.923	0.019
256	-2.964	0.009
512	-2.968	0.008
1024	-2.971	0.007

Table 1: Results of the computation carried out on the microstructure represented in figure 4, for  $E_{12} = 1$ . Although the microstructure is defined on a  $256 \times 256$  grid, the computation can be carried out on coarser or finer grids. The resulting bounds on  $C_{1212}^{\text{eff}}$  improve with the fineness of the computation grid.

The numerical results are gathered in table 1; unsurprisingly, refined computation grids lead to improved bounds on  $C_{1212}^{\text{eff}}$ .

### 3.4 Computation on partially resolved microstructures

The case of partially resolved microstructures is more interesting. Let us assume that the experimental resolution is  $4 \times 4$  pixels, so that the microstructure is observed on a  $64 \times 64$  grid (see figure 4, middle). Then, the mixture of matrix and smallest pores ( $2 \times 2$ ) is seen as a “porous matrix”, with porosity  $\varphi_m$ . It can be verified that with the specific microstructure at hand,  $\varphi_m$  is uniform,  $\varphi_m = 25\%$ . As previously mentioned, it is possible to compute rigorous bounds on the macroscopic elastic moduli of the fully resolved microstructure, provided that rule (5) be applied to each heterogeneous voxel. In the present case, it is found that

$$\mathbf{C}_\beta^h = \mathbf{C}_0 + [(1 - \varphi_m)(\mathbf{C}_m - \mathbf{C}_0)^{-1} - \varphi_m \mathbf{C}_0^{-1}]^{-1}.$$

It should be emphasized that the equivalent stiffness  $\mathbf{C}_\beta^h$  depends on the composition of the heterogeneous voxel  $\beta$  (in the present case, the composition is characterized by  $\varphi_m$ ), not on the spatial repartition of the phases within voxel  $\beta$ . Of course, the latter is out of experimental reach, but the former might be assessed by indirect methods. For example, using microtomography, Scheiner et al. [17] performed an inverse analysis on the measured gray-levels to retrieve the volume fractions of the constituents within each voxel.

Performing the computation on the partially resolved microstructures shown in figure 4 (middle and right) leads to two additional bounds on  $C_{1212}^{\text{eff}}$  which are gathered in table 1. As expected, these bounds are less tight than those obtained on fine grids. However, it is worthwhile emphasizing again that these bounds are rigorous, and might well be the best information that can be retrieved from a resolution-limited experiment.

## 4 Conclusion

In the present paper, two FFT-based homogenization schemes, namely the basic scheme of Moulinec and Suquet [1, 2] and the energy scheme introduced in [5] have been formulated as Galerkin approximations of the same variational problem. It has been shown that these two schemes differ only by the choice of the discrete Green operator. Besides the non-consistent and consistent approximations of this operator, a new one has been proposed, namely the filtered, non-consistent Green operator, the use of which is generally recommended, except when rigorous bounds are required.

For any of the three discrete Green operators discussed in this paper, the discrete variational problem resulting from the Galerkin approximation always has a unique solution, regardless of the stiffness of the reference material. This result must be contrasted with e.g. Michel et al. [7],

where it is proved that the basic scheme converges only for some values of the elastic moduli of the reference material.

This contradiction is in fact only apparent. Indeed, the present approach allowed the distinction between i. the linear system (resulting from the Galerkin discretization) to be solved and ii. the solver used to compute the solution. While the former is always invertible, some choices (such as the Neumann iterations of the basic scheme) might be inappropriate under some circumstances.

Finally, it has been shown that the numerical scheme applies to partially resolved microstructures. In this case of high practical interest, a rule for the computation of the equivalent properties of the heterogeneous voxels has been proposed; application of this rule preserves the status of bound on the effective elastic moduli.

## References

- [1] H. Moulinec and P. Suquet. A fast numerical method for computing the linear and nonlinear properties of composites. *Comptes-rendus de l'Académie des sciences série II*, 318:1417–1423, 1994.
- [2] H. Moulinec and P. Suquet. A numerical method for computing the overall response of nonlinear composites with complex microstructure. *Computer Methods in Applied Mechanics and Engineering*, 157(1-2):69–94, 1998.
- [3] J. Escoda, F. Willot, D. Jeulin, J. Sanahuja, and C. Toulemonde. Estimation of local stresses and elastic properties of a mortar sample by FFT computation of fields on a 3D image. *Cement and Concrete Research*, 41(5):542–556, 2011.
- [4] Ricardo Lebensohn, Anthony Rollett, and Pierre Suquet. Fast fourier transform-based modeling for the determination of micromechanical fields in polycrystals. *JOM Journal of the Minerals, Metals and Materials Society*, 63(3):13–18, 2011.
- [5] S. Brisard and L. Dormieux. FFT-based methods for the mechanics of composites: A general variational framework. *Computational Materials Science*, 49(3):663–671, 2010.
- [6] Z. Hashin and S. Shtrikman. On some variational principles in anisotropic and nonhomogeneous elasticity. *Journal of the Mechanics and Physics of Solids*, 10(4):335–342, 1962.
- [7] J. C. Michel, H. Moulinec, and P. Suquet. A computational scheme for linear and non-linear composites with arbitrary phase contrast. *International Journal for Numerical Methods in Engineering*, 52(1–2):139–160, 2001.
- [8] Sébastien Brisard and Luc Dormieux. Combining Galerkin approximation techniques with the principle of Hashin and Shtrikman to derive a new FFT-based numerical method for the homogenization of composites. *Computer Methods in Applied Mechanics and Engineering*, 217-220(0):197–212, 2012.
- [9] R. Zeller and P. H. Dederichs. Elastic constants of polycrystals. *Physica Status Solidi (B)*, 55(2):831–842, 1973.
- [10] P. Suquet. A simplified method for the prediction of homogenized elastic properties of composites with a periodic structure. *Comptes-rendus de l'Académie des sciences série II*, 311(7):769–774, 1990.

- [11] E. Kröner. Bounds for effective elastic moduli of disordered materials. *Journal of the Mechanics and Physics of Solids*, 25(2):137–155, 1977.
- [12] Alexandre Ern and Jean-Luc Guermond. *Theory and Practice of Finite Elements*, volume 159 of *Applied Mathematical Sciences*. Springer, 2004.
- [13] R. Barrett, M. Berry, T. F. Chan, J. Demmel, J. Donato, J. Dongarra, V. Eijkhout, R. Pozo, C. Romine, and H. Van der Vorst. *Templates for the Solution of Linear Systems: Building Blocks for Iterative Methods*. SIAM, 2 edition, 1994.
- [14] C. C. Paige and M. A. Saunders. Solution of sparse indefinite systems of linear equations. *SIAM Journal of Numerical Analysis*, 12(4):617–629, 1975.
- [15] Christopher C. Paige and Michael A. Saunders. LSQR: An algorithm for sparse linear equations and sparse least squares. *ACM Transactions on Mathematical Software*, 8(1): 43–71, 1982.
- [16] J. R. Willis. Bounds and self-consistent estimates for the overall properties of anisotropic composites. *Journal of the Mechanics and Physics of Solids*, 25(3):185–202, 1977.
- [17] Stefan Scheiner, Raffaele Sinibaldi, Bernhard Pichler, Vladimir Komlev, Chiara Renghini, Chiara Vitale-Brovarone, Franco Rustichelli, and Christian Hellmich. Micromechanics of bone tissue-engineering scaffolds, based on resolution error-cleared computer tomography. *Biomaterials*, 30(12):2411–2419, 2009.